Activation of transient receptor potential vanilloid 1 (TRPV1) by resiniferatoxin

Manish Raisinghani, Reddy M. Pabbidi and Louis S. Premkumar

Department of Pharmacology, Southern Illinois University School of Medicine, Springfield, IL-62702, USA

Transient receptor potential vanilloid 1 (TRPV1) is a Ca^{2+} permeable non-selective cation channel activated by physical and chemical stimuli. Resiniferatoxin (RTX), an ultrapotent agonist of TRPV1, is under investigation for treatment of urinary bladder hyper-reflexia and chronic pain conditions. Here, we have determined the characteristics of RTX-induced responses in cells expressing native and cloned rat TRPV1. Whole-cell currents increase with repeated application of submaximal concentrations of RTX until a maximal response is attained and do not deactivate even after prolonged washout. Interestingly, the rate of activation and block by capsazepine of RTX-induced currents are significantly slower than for capsaicin-induced currents. RTX-induced whole-cell currents are outwardly rectifying, but to a lesser extent than capsaicin-induced currents. RTX-induced single channel currents exhibit multiple conductance states and outward rectification. The open probability (P_o) of RTX-induced currents is higher at all potentials as compared to capsaicin-induced currents, which showed a strong voltage-dependent decrease at negative potentials. Single-channel kinetic analyses reveal that open-time distribution of RTX-induced currents can be fitted with three exponential components at negative and positive potentials. The areas of distribution of the longer open time constants are significantly larger than capsaicin-induced currents. The closed-time distribution of RTX-induced currents can be fitted with three exponential components as compared to capsaicin-induced currents, which require four exponential components. Current-clamp experiments reveal that low concentrations of RTX caused a slow and sustained depolarization beyond threshold while generating few action potentials. Concentrations of capsaicin required for the same extent of depolarization generated a significantly greater number of action potentials. These properties of RTX may play a role in its clinical usefulness.

(Resubmitted 31 March 2005; accepted after revision 18 July 2005; first published online 21 July 2005)
Corresponding author L. S. Premkumar: Department of Pharmacology, Southern Illinois University School of Medicine, Springfield, IL-62702, USA. Email: lpremkumar@siumed.edu

Transient receptor potential vanilloid 1 (TRPV1/VR1) is a non-selective cation channel with high calcium permeability expressed on the peripheral and central terminals of small-diameter sensory neurones (Caterina *et al.* 1997; Dinh *et al.* 2004; Lazzeri *et al.* 2004*c*). It functions as a polymodal nociceptor at the peripheral nerve terminals and modulates synaptic transmission at the first sensory synapse between dorsal root ganglion (DRG) and dorsal horn neurones (Nakatsuka *et al.* 2002; Baccei *et al.* 2003). TRPV1 has also been shown to modulate synaptic transmission in certain regions of the brain (Doyle *et al.* 2002; Marinelli *et al.* 2002, 2003). TRPV1 is activated by heat ($> 42^{\circ}$C), capsaicin (pungent ingredient of hot chilli peppers), resiniferatoxin (RTX), protons, anandamide, arachidonic acid metabolites and *N*-arachidonyl dopamine (NADA) (Szallasi & Blumberg, 1990*a*,*b*; Caterina *et al.* 1997; Zygmunt *et al.* 1999; Hwang *et al.* 2000; Julius & Basbaum, 2001; Caterina & Julius, 2001; Chuang *et al.* 2001; De Petrocellis *et al.* 2001; Huang *et al.* 2002). RTX, derived from *Euphorbia resinifera* is the most potent amongst all the known endogenous and synthetic agonists for TRPV1. The tritiated form (^{3}[H]RTX) has been used as a tool in ligand-binding assays (Szallasi & Blumberg, 1990*b*; Roberts *et al.* 2004). Binding of capsaicin and RTX to TRPV1 involves amino acid residues which have been shown to reside in N- and C-cytosolic and transmembrane domains of the channel (Jung *et al.* 1993, 2002; Chou *et al.* 2004; Gavva *et al.* 2004). RTX combines structural features of phorbol esters (potent activators of protein kinase C (PKC)) and vanilloid compounds. It was thought that its ability to activate PKC might be responsible for its high potency, but the concentration required to activate PKC is much higher than needed to account for this effect (Harvey *et al.* 1995).

 DOI: 10.1113/jphysiol.2005.087874

TRPV1 is implicated in inflammatory thermal sensitivity, as TRPV1 knockout mice are able to sense normal temperature with some deficiency, but lack thermal hypersensitivity following inflammation (Caterina *et al.* 2000; Davis *et al.* 2000). Although TRPV1 is mainly considered to be involved in thermal sensory perception, its distribution in regions that are not exposed to such temperatures raises the possibility of functions other than detection of heat. TRPV1 can be detected using RT-PCR and radioligand binding throughout the neuro-axis, and identification of specific ligands such as NADA in certain brain regions further suggests possible roles in the CNS (Huang *et al.* 2002; Szabo *et al.* 2002; Zheng *et al.* 2003; Vass *et al.* 2004). TRPV1 is present in the blood vessels and bronchi where activation of this receptor leads to potent vasodilatation (by releasing calcitonin gene-related peptide (CGRP)) and bronchoconstriction, respectively (Lundberg *et al.* 1983; Mitchell *et al.* 1997; Oroszi *et al.* 1999). TRPV1 is found in the nerve terminals supplying the bladder and the urothelium, where activation may have a role in bladder function, including micturition (Birder *et al.* 2002; Linard *et al.* 2003; Dinis *et al.* 2004).

Recently, RTX has found therapeutic usefulness and is undergoing clinical trials for the treatment of bladder hyper-reflexia (Lazzeri *et al.* 1998; Kim *et al.* 2003). Single intravesicular administration of RTX produces a long-lasting improvement of this condition (Cruz *et al.* 1997; Lazzeri *et al.* 1998; Brady *et al.* 2004; Karai *et al.* 2004). It has also been found that RTX is useful in painful conditions affecting joints where its injection into the joint cavity has led to a dramatic improvement in joint mobility by reducing pain (Helyes *et al.* 2004). The rationale for RTX treatment is believed to arise from a combination of Ca^{2+}-dependent desensitization and the nerve terminals undergoing cell death from excessive influx of Ca^{2+} via TRPV1. The long-lasting effect of RTX supports the latter as a more likely mechanism of action as shown by the effect of RTX administration into the bladder of patients with bladder hyper-reflexia (Brady *et al.* 2004). It has been documented that intravesicular application of RTX, unlike capsaicin, does not induce suprapubic discomfort (Giannantoni *et al.* 2004). Findings from this study show that even at low concentrations RTX is able to activate TRPV1 slowly with high potency, which might result in a sustained increase in intracellular Ca^{2+} without generating action potentials, leading to nerve terminal death.

In this study we have found, using whole-cell and single-channel recordings, that RTX induced slow, sustained and irreversible current. In current-clamp experiments, lower concentrations of RTX induced slow and sustained membrane depolarization, but exhibited a lesser propensity to generate action potentials than capsaicin.

Methods

Electrophysiology

Whole-cell and single-channel currents were recorded from rat DRG neurones in culture and from *Xenopus laevis* oocytes injected with rat TRPV1 cRNA. Animals were cared for according to the standards of the National Institutes of Health (NIH). All animal use protocols were approved by Southern Illinois University School of Medicine Animal Care Committee.

Oocytes were obtained by an abdominal incision after anaesthetizing the frog by immersion in a 0.05% solution of 3-aminobenzoic acid ethyl ester (MS222). Animals were killed by a subcutaneous injection of a 2% solution of MS222 according to NIH guidelines. One day after separating the oocytes from the follicular layer, 50–70 nl TRPV1 cRNA was injected using a Drummond Nanoject (Drummond Scientific Co., Broomall, PA, USA). Oocytes were used for recording from 3 days after the injection. Double-electrode voltage clamp was performed using a Warner amplifier (Warner Instruments, Hamden, CT, USA). Data were digitized and stored on videotape or directly stored on the computer using a LabView interface (National Instruments, Austin, TX, USA). Experiments were performed at 21–23°C. Oocytes were placed in a Perspex chamber superfused (5–10 ml min^{-1}) with Ca^{2+}-free Ringer solution containing (mM): NaCl 100, KCl 2.5 and Hepes 5; pH adjusted to 7.35 with NaOH. Current–voltage relationships were measured using 1-s voltage ramps from −80 to +80 mV.

Primary DRG neuronal cultures were prepared from embryonic day 18 (E18) rat embryos. Adult pregnant rats were killed with an overdose of isoflurane. DRG were dissected and the cells were dissociated by triturating with a fire-polished glass pipette. Cells were cultured in Neurobasal medium (Life Technologies, Buffalo, NY, USA), supplemented with 10% fetal bovine serum (FBS), and grown on poly-D-lysine-coated glass coverslips. Cells were used from 5 to 15 days after plating. Small diameter ($< 30\ \mu m$) rounded neurones were selected for patch-clamp experiments. More than 70% of the neurones responded to capsaicin. The Giga-seal patch-clamp technique was used to record whole-cell currents. For perforated-patch recordings, the bath solution contained (mM): sodium gluconate 140, KCl 2.5, Hepes 10, $MgCl_2$ 1 and EGTA 1.5 (pH adjusted to 7.35 with NaOH), and the pipette solution contained (mM): sodium gluconate 130, NaCl 10, KCl 2.5, Hepes 10, $MgCl_2$ 1, EGTA 1.5 and 240 $\mu g\ ml^{-1}$ amphotericin B (pH adjusted to 7.35 with NaOH). For current-clamp experiments the pipette solution contained (mM): potassium gluconate 130, NaCl 10, $MgCl_2$ 1, EGTA 0.2, K_2ATP 1 and Hepes 10; pH adjusted to 7.35 with NaOH. Extracellular solution for current- and voltage-clamp experiments contained (mM):

NaCl 140, KCl 4, $MgCl_2$ 1 and Hepes 10; pH adjusted to 7.35 with NaOH. Currents were recorded using a WPC 100 patch-clamp amplifier (E.S.F. Electronic, Goettingan, Germany). Data were filtered at 10 kHz, digitized (VR-10B, Instrutech Corp., Great Neck, NY, USA) and stored on videotapes or directly stored in the computer using a LabView interface. For analysis of whole-cell currents, data were filtered at 1 kHz (−3db frequency with an 8-pole low-pass Bessel filter, Warner Instruments, LPF-8) and digitized at 2 kHz.

For single-channel recording in cell-attached patches from DRG neurones, the bath solution contained (mM): potassium gluconate 140, KCl 2.5, $MgCl_2$ 1, Hepes 5 and EGTA 1.5; pH adjusted to 7.35 with NaOH. The patch pipettes were made from glass capillaries (Drummond, Microcaps), coated with Sylgard (Dow Corning, Midland, MI, USA). For cell-attached patches, the patch pipettes were filled with a solution that contained (mM): sodium gluconate 140, NaCl 10, $MgCl_2$ 1, Hepes 5 and EGTA 1.5; pH adjusted to 7.35 with NaOH. While recording from cell-attached patches, in order to avoid differences in the driving force because of the differences in the membrane potential, the external NaCl was replaced by an equal amount of KCl in order to nullify the membrane potential. For outside-out patches, the pipette solution contained (mM): sodium gluconate 90, NaCl 10, BAPTA 10, Hepes 10, K_2ATP 2 and GTP 0.25; pH adjusted to 7.35 with NaOH. The bath solution contained (mM): sodium gluconate 100, KCl 2.5, $MgCl_2$ 1, Hepes 5 and EGTA 1.5; pH adjusted to 7.35 with NaOH. All the experiments were performed at room temperature (21–23°C). Agar-bridge electrodes were used to avoid changes in junction potential. The currents were recorded using a WPC 100 (Warner Instruments) or Axopatch 2B (Axon Instruments, Union City, CA, USA) patch-clamp amplifier. Data were filtered at 10 kHz (Axopatch 2B), digitized (VR-10B, Instrutech Corp.), and stored on videotapes. For the analysis of amplitude and open probability (P_o), the data were filtered at 2.5 kHz (−3db frequency with an 8-pole low-pass Bessel filter, Warner Instruments) and digitized at 5 kHz. For dwell-time analysis, the data were filtered at 10 kHz and digitized at 50 kHz.

Single-channel analyses

Single-channel current amplitude and P_o were estimated from all-point current amplitude histograms (Channel 2 software kindly provided by Michael Smith, Australian National University, Canberra, Australia) and fitted to Gaussian densities (Origin, OriginLab Corp., Northampton, MA, USA). For current–voltage relationships, the amplitudes were determined by fitting a Gaussian curve to an all-point histogram. P_o was determined using unedited segments of data, which were typically 1–5 min long. For multiple channel patches, the mean P_o was measured as nP_o, where n is the number of channels in the patch. Chord conductance was measured at +60 or −60 mV. Slope conductance was determined by linear fits to current–voltage data between +20 and +100 mV or −20 and −100 mV.

Patches that apparently had a single TRPV1 channel (assessed by the lack of overlapping events at +60 mV, when the P_o was > 0.7) were used for dwell-time analysis. Single-channel currents were idealized using a modified Viterbi algorithm (QUB software, www.qub.buffalo.edu). Dwell-time distributions were fitted with mixtures of exponential densities using a method of maximum likelihood. Additional exponential components were incorporated only if the maximum log likelihood increased more than 2 log likelihood units (Chung *et al.* 1990; Qin *et al.* 1996; Premkumar *et al.* 1997). A dead time (τ_d) of 50 μs was imposed retrospectively, in that, events shorter than 50 μs were considered to be a part of the adjoining sojourns.

All the chemicals used in this study were obtained from Sigma (St Louis, MO, USA). The working concentrations of the drugs were freshly prepared from the following ethanol stock solutions: RTX (100 mM), capsaicin (100 mM) and capsazepine (50 mM). The final solution contained $< 0.001\%$ ethanol. Data are given as mean ± S.E.M and statistical significance was evaluated using the Student's t test.

Results

Activation of whole-cell currents in oocytes by RTX

Whole-cell currents were recorded from oocytes heterologously expressing TRPV1. At a holding potential of −60 mV, application of capsaicin (300 nM), protons (pH 5.5), NADA (10 μM) and RTX (10 nM) induced inward currents. NADA is a weak agonist and did not induce a maximal response even at a concentration of 10 μM. The currents induced by capsaicin, protons and NADA could be reversed readily when the agonists were removed (Fig. 1*A*–*C*). In contrast, RTX-induced currents did not deactivate even after a prolonged washout (> 15 min) (Fig. 1*D*). Qualitatively, it is clear that the activation and deactivation phases are different for RTX-induced currents as compared to currents activated by capsaicin, protons and NADA. (Fig. 1*A*, *B* and *C*). RTX-induced currents are activated slowly and minimally deactivated (Fig. 1*D* and *E*). Moreover, repeated application of a submaximal concentration of RTX (10 nM) induced larger currents until a maximal response was attained; the current could be readily blocked by ruthenium red (100 μM) (Fig. 1*E*). To quantify the differences in activation phase, we measured the activation time (10–90% of the rising phase) and the summary graph shows that the activation phase of RTX-induced currents is two-fold slower than capsaicin-induced (300 nM)

and proton-induced (pH 5.5) currents (capsaicin, 23.9 ± 1.5 s, $n = 11$; protons, 20.2 ± 0.7 s, $n = 11$; RTX, 61.4 ± 4.4 s, $n = 13$) (Fig. 1*F*). A ramp protocol, which changed the voltage from −80 to +80 mV in 1 s, was used to determine the current–voltage relationship of the responses induced by RTX (10 nM) and capsaicin (300 nM) (Fig. 1*G*). Agonist-induced currents are shown after subtracting the leak current in the absence of the agonist. Capsaicin- and RTX-induced currents reversed at -12.3 ± 0.42 ($n = 3$) and -10.4 ± 0.53 ($n = 4$) mV, respectively. Although an outward rectification pattern was seen with both agonists, RTX-induced currents showed a lesser degree of outward rectification. In order to quantify this, we calculated the ratio of outward and inward currents. The ratio was significantly larger ($P < 0.05$) for capsaicin-induced (6.6 ± 1.3, $n = 6$) as compared to RTX-induced (2.35 ± 0.97, $n = 3$) currents. Although, increasing concentrations of RTX induced larger currents, repeated application of the same sub-maximal concentration also induced larger currents. Thus, it was difficult to construct a meaningful dose–response curve for RTX. Repeated application of agonists such as capsaicin, protons, NADA and anandamide increases the amplitude of the current in oocytes and DRG neurones; in the case of NADA and anandamide this has been attributed to activation of PKC. PKC activation increases sensitivity as well as TRPV1 translocation (Van Buren *et al.* 2005). A similar phenomenon could play a role in the observation of increased current amplitude with repeated application of low concentrations of RTX (Premkumar *et al.* 2004). It is also possible that RTX is partitioned in the membrane and repeated application can increase the availability of RTX for binding. In the past, an EC_{50} value (39 nM) has been obtained by applying increasing concentrations of RTX; however, results from this study suggest that a dose–response curve does not give an accurate determination of the EC_{50} value, but it does confirm the ultra potency of RTX as shown in previous studies (Szallasi & Blumberg, 1990*b*; Caterina *et al.* 1997; Marshall *et al.* 2003).

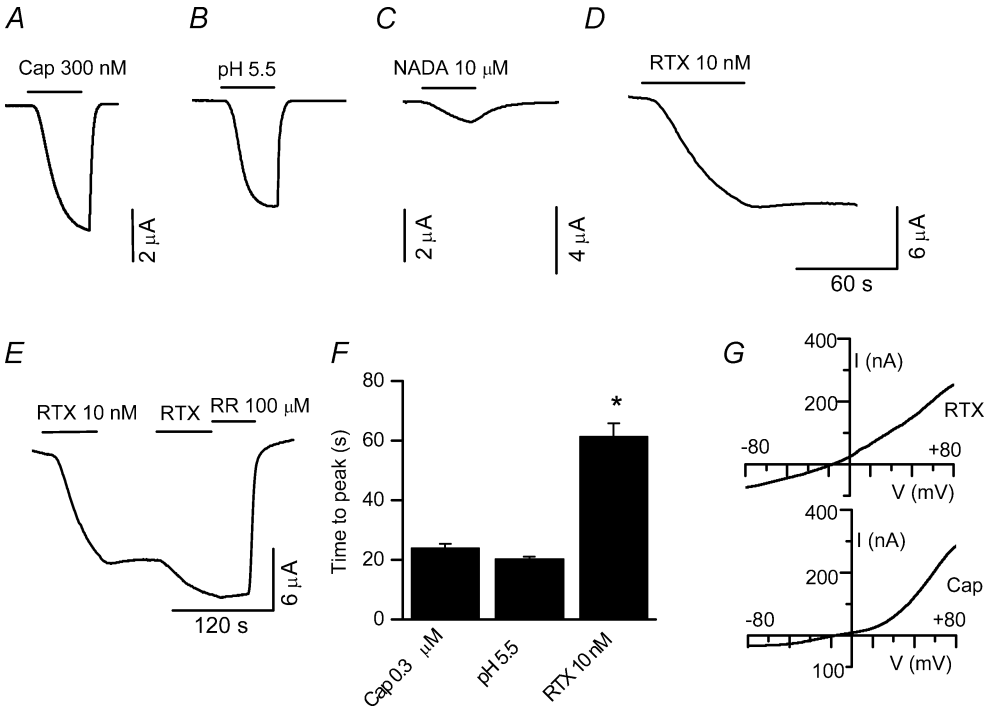

Figure 1. Cloned TRPV1-mediated whole-cell currents in oocytes
Currents activated by 1 μM capsaicin (*A*), pH 5.5 (*B*), 10 μM NADA (*C*) and 10 nM RTX (*D*). *E,* note that the RTX-induced current does not deactivate. Repeated application of a submaximal concentration of RTX (10 nM) induced larger currents, which could be completely blocked with 100 μM ruthenium red (RR). *F*, summary graph showing that the time to reach the peak (10–90%) current is ∼ three times longer in the presence of RTX as compared to the other agonists. $^*P < 0.05$. *G*, current generated by a ramp protocol from −80 to +80 mV in the presence of RTX (top trace) and capsaicin (Cap, bottom trace) shows a lesser degree of rectification of RTX-induced currents.

Activation of whole-cell current in DRG neurones by RTX

Next we determined the properties of RTX-induced membrane currents on native TRPV1 in embryonic DRG neurones grown in culture. The cells were voltage-clamped at −60 mV and currents were evoked by RTX and capsaicin. Protons were not used to elicit currents because of the presence of acid-sensitive ion channels in these neurones. Capsaicin-induced (1 μM) currents were readily reversible. However, as previously observed in oocytes (Fig. 1*D*), RTX (10 and 100 nM) induced a sustained current that could not be reversed readily even after a prolonged washout (> 15 min) (Fig. 2*A*). Furthermore, capsaicin-induced currents exhibited a relatively fast activation and deactivation phase, whereas RTX-induced currents exhibited significantly slower activation phase as compared to capsaicin-induced currents (RTX 10 nM, 69 ± 10.9, $n = 6$; RTX 100 nM, 29.35 ± 2.65 s, $n = 6$; capsaicin 1 μM, 7.14 ± 0.42 s, $n = 66$) ($P < 0.001$, Fig. 2*A* and *B*). We did not observe any difference in the activation kinetics of RTX-induced currents with or without prior application of capsaicin.

We determined the block of TRPV1 current induced by RTX and capsaicin by a competitive TRPV1 blocker. Capsazepine (10 μM) completely blocked the current induced by capsaicin (1 μM) and RTX (10 nM). However, the rate of block induced by capsazepine was significantly slower (612.3 ± 219 s, $n = 6$) for RTX-induced currents than for capsaicin-induced currents (18.4 ± 2.8 s, $n = 10$) (Fig. 2*C–E*, $P < 0.01$). These experiments suggest that even though RTX binds to TRPV1 with high affinity, it is unable to activate the receptor rapidly and deactivates minimally.

Single-channel currents activated by RTX and capsaicin in native and cloned TRPV1

Single-channel conductance. To further evaluate the properties of TRPV1 activation by RTX, we recorded single-channel currents from cell-attached and excised patches from DRG neurones and oocytes heterologously expressing TRPV1. All recordings were carried out in the absence of extracellular calcium to avoid tachyphylaxis and desensitization of channel activity (Docherty *et al.* 1996; Caterina *et al.* 1997; Koplas *et al.* 1997). Single-channel current activity in cell-attached patches from DRG neurones were recorded at −60 and +60 mV, as shown in Fig. 3. Single-channel current amplitude of RTX-induced currents was 2.3 ± 0.21 pA ($n = 8$) at −60 mV and 6.02 ± 0.14 pA ($n = 6$) at +60 mV

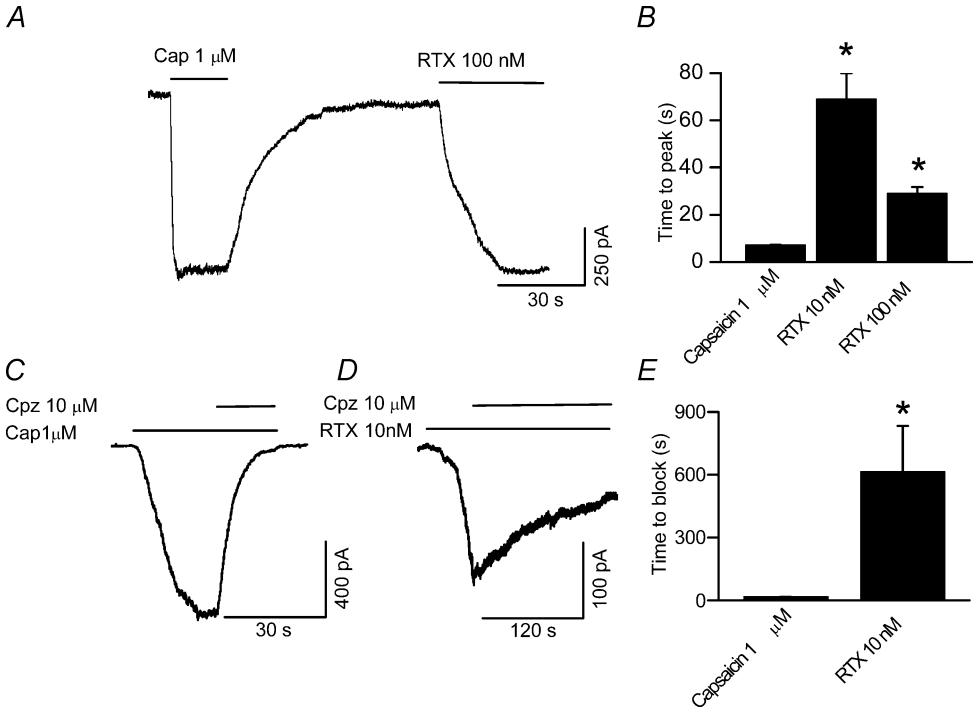

Figure 2. TRPV1-mediated whole-cell currents in DRG neurones
A, RTX-induced (100 nM) current exhibits a significantly longer time to peak than capsaicin-induced (1 μM) current and deactivates minimally. *B*, summary graph showing significantly longer time to peak for RTX- than for capsaicin-induced currents. *C*, *D* rate of block of RTX-induced currents by capsazepine (10 μM) is significantly slower than block of capsaicin-induced currents. *E*, summary graph showing significantly longer time taken for capsazepine to block RTX- than capsaicin-induced currents.

corresponding to a conductance of 38.3 ± 3.5 pS and 100 ± 2.2 pS, respectively (Fig. 3*A*). Although RTX is a potent agonist, single-channel conductance is lower at negative potentials as compared to positive potentials. In comparison to RTX-induced currents, single-channel currents induced by capsaicin (100 nM) had amplitudes of 2.4 ± 0.12 ($n = 10$) and 5.67 ± 0.06 pA ($n = 10$) at -60 and $+60$ mV corresponding to conductances of 40 ± 1.95 and 95 ± 0.1 pS, respectively (Fig. 3*B*, also see Premkumar *et al.* 2002).

Next we recorded single-channel currents from the cloned TRPV1 in excised patches. RTX-induced current amplitudes were 2.59 ± 0.17 and 6.19 ± 0.05 pA ($n = 6$) corresponding to conductances of 43 ± 2.8 and 103.3 ± 0.83 pS, at -60 and $+60$ mV, respectively (Fig. 4*A*). Capsaicin-induced current amplitudes were 2.52 ± 0.08 ($n = 27$) and 5.71 ± 0.1 pA ($n = 28$) corresponding to conductance of 41.8 ± 1.3 and 95.3 ± 1.7 pS at -60 mV and $+60$ mV, respectively, as previously described (Premkumar *et al.* 2002) (Fig. 4*B*)

Careful analysis of single-channel currents induced by RTX revealed multiple conductance states. Both, supra- and subconductance states were observed (Fig. 5*A* and *B*). In comparison to capsaicin-induced currents, which predominantly dwelled at a conductance level of ~95 pS, RTX-induced currents showed multiple conductance states. In DRG neurones at +60 mV, the current amplitudes were 3.2, 5.2 and 6.9 pA, corresponding to conductance levels of 53, 86 and 115 pS, respectively (Fig. 5*A*). In oocytes expressing TRPV1, at +60 mV, RTX-induced currents had amplitudes of 3.5, 5.3 and 6.9 pA, corresponding to single-channel conductance of 58, 88 and 115 pS, respectively (Fig. 5*B*).

Current–voltage relationship and rectification. RTX- and capsaicin-induced channel activity were recorded from -100 to $+100$ mV (Fig. 6). Several studies have shown that the whole-cell current–voltage relationship for TRPV1 exhibits a profound outward rectification (Caterina *et al.* 1997; Tominaga *et al.* 1998; Premkumar *et al.* 2002). For RTX-induced currents, the polarity of single-channel currents reversed close to 0 mV (-2.9 mV, $n = 2$). The outward limb of the single-channel current–voltage relationship has a slope conductance of 126 pS (between 0 and +100 mV) and the inward current limb has a slope conductance of ~30 pS (between 0 and -100 mV) (Fig. 6*A* and *B*). At negative potentials, single-channel conductance did not change linearly with voltage beyond -60 mV,

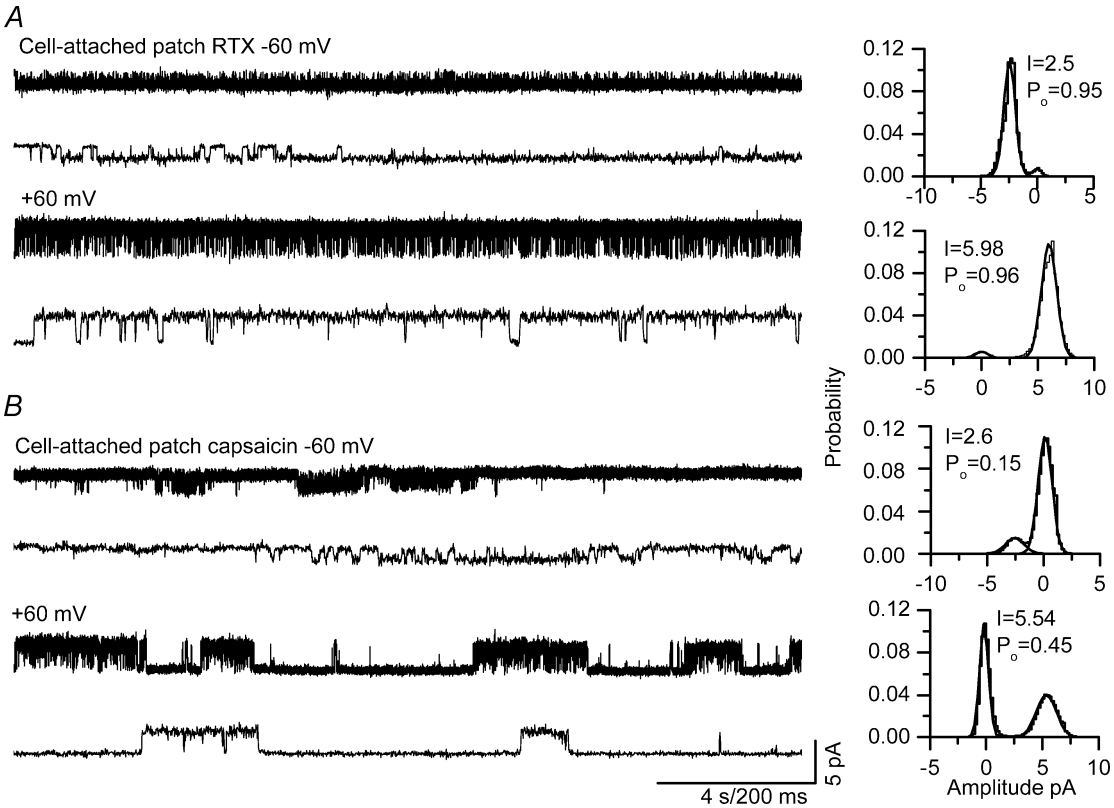

Figure 3. Single-channel current recordings in cell-attached patches from DRG neurones
A, RTX-induced (0.1 nM) single-channel activity at -60 and +60 mV. *B*, capsaicin-induced (100 nM) single-channel activity at -60 and +60 mV. The corresponding all-point amplitude histograms are shown on the right. Lower traces show single-channel recordings at a higher time resolution.

whereas at positive potentials the current–voltage curve was ohmic. We do not have a good explanation for this observation. Similar to previous studies, this study showed that the slope conductance of capsaicin-induced currents is 41 pS at negative potentials as compared to 107 pS at positive potentials (Fig. 7*A* and *B*). Single-channel conductance is lower at negative than at positive potentials and increased linearly with voltage at both negative and positive potentials. Even though RTX is a potent activator, the current–voltage relationship is not linear, suggesting that the difference in conductance is an inherent property of the receptor. The difference in single-channel conductance is partly responsible for the outward rectification, but to a lesser extent as compared to capsaicin-induced currents, which also exhibits is due to a lack of voltage-dependent change in P_o as described below.

Single-channel open probability (P_o). Single-channel activity of RTX-induced currents in cell-attached patches as well as outside-out patches exhibited a high P_o (∼0.9) (Figs 3*A*, 4*A* and 6*A*). Single-channel P_o did not change with increasing concentrations of RTX from 0.1 to 20 nM. Only the time to attain maximum P_o was longer when lower concentrations of RTX were used. Thus, all single-channel analyses for RTX-induced activation of TRPV1 were performed in the presence of 0.1–0.2 nM RTX. Moreover, there is no voltage-dependent change in P_o, unlike capsaicin-induced currents. At both negative and positive potentials, the P_o was ∼0.9 (Figs 3*A*, 4*A*, and 6*A* and *C*). Single channel P_o was 0.94 ± 0.02 ($n = 6$) and 0.98 ± 0.02 ($n = 3$) at −60 and +60 mV, respectively, in cell-attached patches from DRG neurones (Fig. 3*A*). Next we recorded single-channel currents using outside-out patches from oocytes expressing TRPV1. In the presence of RTX, the P_o was high: 0.83 ± 0.05 ($n = 3$) and 0.88 ± 0.03 ($n = 3$) at −60 and +60 mV, respectively (Fig. 4*A*). Even in excised patches, RTX-induced P_o is higher than capsaicin-induced P_o.

Application of capsaicin showed a concentration-dependent increase and a voltage-dependent decrease in P_o at negative potentials (Premkumar *et al.* 2002). In cell-attached patches, the P_o in the presence of 100 nM capsaicin at −60 and +60 mV was 0.1 ± 0.04 ($n = 6$)

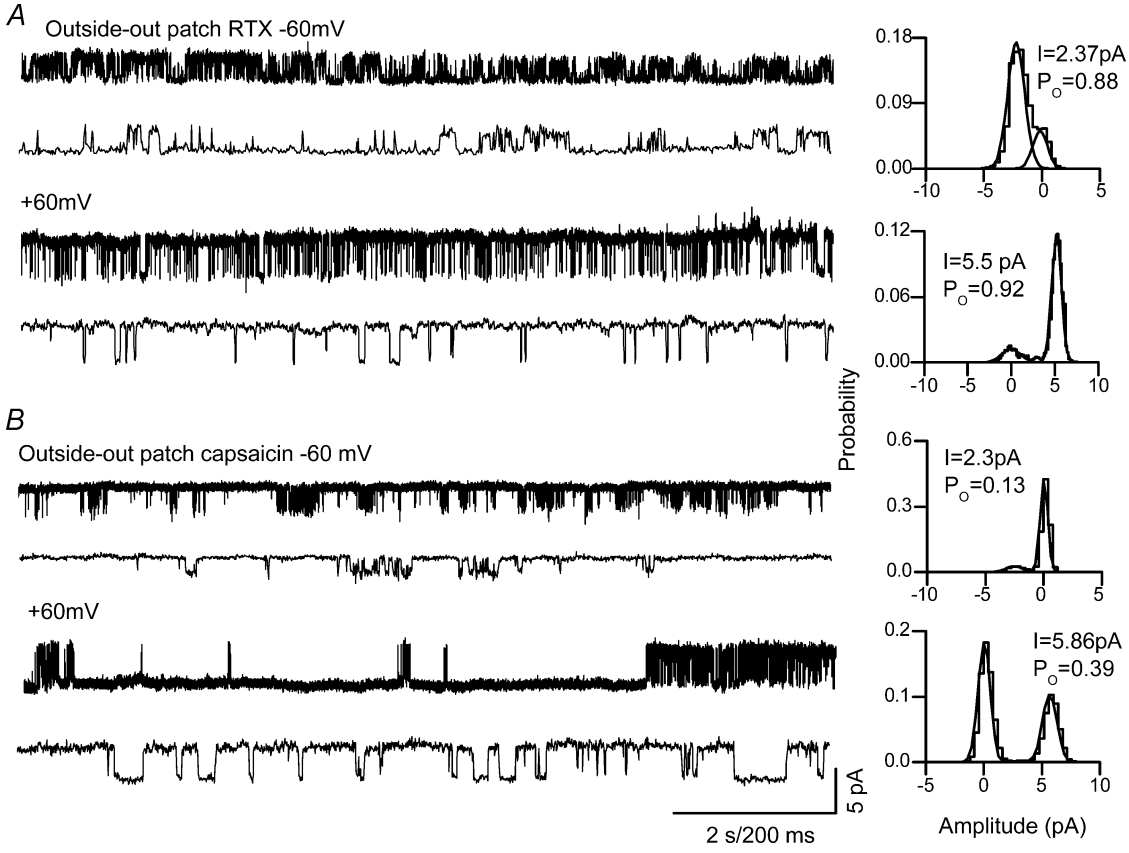

Figure 4. Single-channel current recordings in an excised patch from oocytes injected with cRNA for TRPV1

A, RTX-induced (0.1 nM) single-channel activity at −60 and +60 mV. *B*, capsaicin-induced (100 nM) single-channel activity at −60 and +60 mV. The corresponding all-point amplitude histograms are shown on the right. Lower traces show the single-channel recordings at a higher time resolution.

and 0.53 ± 0.04 ($n = 7$), respectively (Figs 3*B*, 4*B* and 7*A* and *C*). Similarly, in excised patches the P_o in the presence of 100 nM capsaicin at -60 and $+60$ mV was 0.14 ± 0.01 ($n = 34$) and 0.4 ± 0.03 ($n = 38$), respectively. The maximal P_o in the presence of 1 μM capsaicin was 0.8 ± 0.04 and 0.4 ± 0.08 in cell-attached patches at -60 and $+60$ mV, respectively, as reported in a previous study (Premkumar *et al.* 2002). Even at high concentrations of capsaicin, the voltage-dependent change in P_o at negative potentials was apparent. Moreover, capsaicin-induced TRPV1 channel activity was reversible even at higher concentrations, unlike the irreversible nature of activation observed with RTX (data not shown), which was consistent with the observation in whole-cell experiments.

Single-channel kinetics of RTX- and capsaicin-induced channel activity. Single-channel kinetic analyses were carried out from patches that apparently had one channel, using the criterion of non-overlapping events when the P_o was > 0.7. The data (stretches ≥ 1 min) were first idealized using a single open and closed state. This was followed by incorporation of additional open and closed states until the dwell-time histograms were well-fitted with a mixture of exponential densities. Method of maximal log likelihood was used to determine the best fit for the data. Additional states were incorporated only if the log likelihood increased by at least 2 log units. Analyses of single-channel kinetics of TRPV1 currents activated by RTX exhibited no voltage-dependent behaviour, unlike capsaicin-induced currents. (Table 1, Fig. 8).

The open-time distribution of RTX-induced (0.1–0.2 nM) single-channel currents recorded in DRG neurones could be well-fitted with three exponential components (Fig. 8*A* and Table 1). Increasing the concentration of RTX did not change the time constants or their relative areas of distribution, unlike with capsaicin (Premkumar *et al.* 2002). This finding is consistent with the observation that P_o is independent of the concentration. The mean open-time constants and their relative areas of distribution (in parentheses) in the presence of RTX at -60 mV in cell-attached patches were 0.46 ± 0.1 ms (0.03 ± 0.01), 5.57 ± 2.4 ms (0.5 ± 0.3) and 10.2 ± 1.8 ms (0.47 ± 0.3) ($n = 6$). The mean open-time constants and their relative areas of distribution at $+60$ mV were 1.6 ± 1.2 ms (0.11 ± 0.1), 6.58 ± 0.56 ms (0.72 ± 0.12) and 12 ± 1 ms (0.25 ± 0.01) ($n = 3$). (Fig. 8*A* right panel and Table 1). The mean open times of RTX-induced currents are 7.5 ms and 7.9 ms at

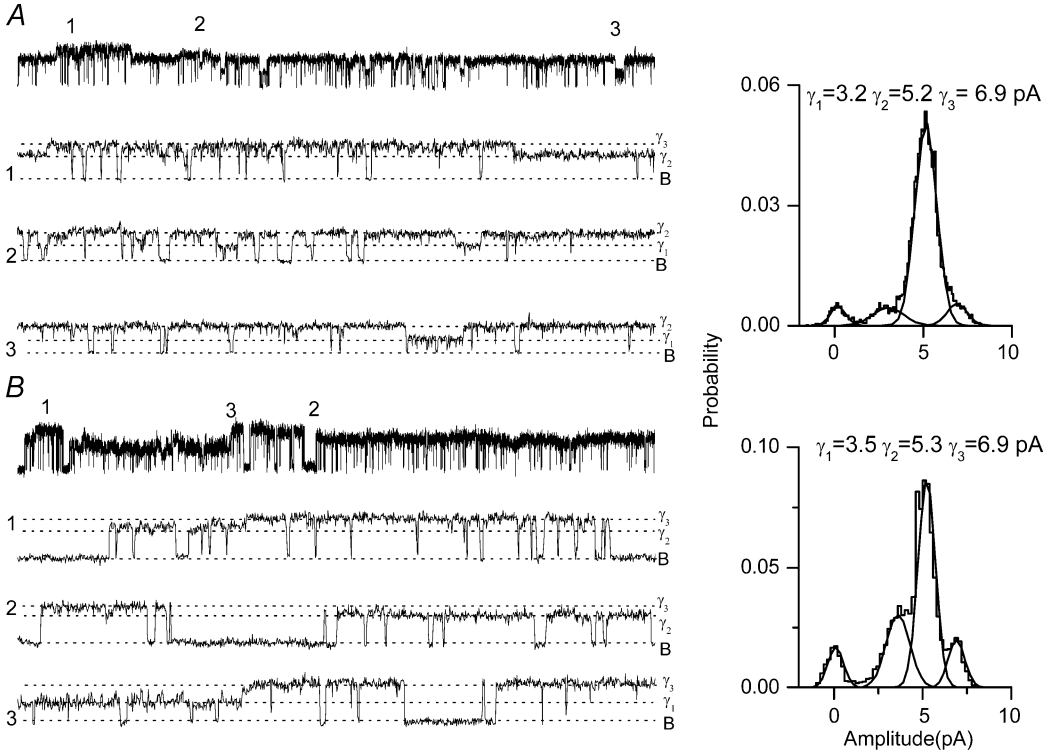

Figure 5. Multiple conductance states of RTX-induced TRPV1 currents
A, selected segments of single-channel currents recorded in a cell-attached patch from a DRG neurone at +60 mV with 0.1 nM RTX in the patch pipette. *B*, selected segment of single-channel currents recorded in cell-attached patch from an oocyte expressing TRPV1 at +60 mV. Regions denoted 1, 2, 3 represent characteristic supra and subconductance states. All-point amplitude histograms showing the conductance levels and their relative frequency of occurrence from selected regions are on the right.

−60 and +60 mV, respectively. From these analyses, it is clear that RTX-induced currents dwelled predominantly in long open states.

For capsaicin-induced currents, at negative potentials (−60 mV), three exponential components were required to fit the open-time distributions. The mean open-time constants and their relative areas of distribution at −60 mV were 0.11 ± 0.01 (0.26 ± 0.05), 0.76 ± 0.18 (0.49 ± 0.07), 2.61 ± 0.84 (0.34 ± 0.08) ($n = 6$). At positive potentials four exponential components were required. The mean open-time constants and their relative area of distribution at +60 mV were 0.14 ± 0.04 (0.11 ± 0.02), 0.7 ± 0.13 (0.28 ± 0.03), 3.83 ± 0.62 (0.44 ± 0.02) and 14.7 ± 2.6 (0.13 ± 0.03) ($n = 7$) (Fig. 8*B* right panel and Table 1). The mean open times of capsaicin-induced currents are 1.27 and 3.8 ms at −60 and +60 mV, respectively. It is clear from this analyses that in the presence of RTX, the open-time distributions and the mean open time did not show any voltage dependence, unlike in the presence of capsaicin. Also, in the presence of capsaicin the mean open times are shorter at −60 and +60 mV.

In most of the patches, the closed-time distribution of RTX-induced currents could be well-fitted with three exponential components. The fractional area of the third exponential component was negligible (Fig. 8*A* left panel and Table 1). The closed-time constants and their fractional area of distribution at −60 mV in cell-attached patches were 0.05 ± 0.007 (0.47 ± 0.02), 0.12 ± 0.005 (0.5 ± 0.02), 1.1 ± 0.26 (0.01 ± 0.002) ($n = 6$). The closed-time constants and their relative area of distribution at +60 mV in cell-attached patches were 0.1 ± 0.008 (0.89 ± 0.02), 0.46 ± 0.02 (0.08 ± 0.01) and 8.7 ± 3.9 (0.01 ± 0.01) ($n = 3$) (Fig. 8*A* left panel and Table 1).

In the presence of capsaicin the closed-time distribution was well fitted with four exponential components (Fig. 8*B* left panel and Table 1). The time constants of the two shortest exponential components changed minimally, if at all, with capsaicin concentration, suggesting that these components reflect fully liganded shut states. At −60 mV, the mean closed-time constants and their relative area of distribution were 0.13 ± 0.02 (0.43 ± 0.04), 0.79 ± 0.12 (0.31 ± 0.03), 3.47 ± 0.59 (0.19 ± 0.03) and 30.8 ± 12.4 (0.04 ± 0.02). At +60 mV, the mean closed-time constants and their relative areas of distribution were 0.06 ± 0.02 (0.39 ± 0.04), 0.67 ± 0.39 (0.4 ± 0.03), 1.66 ± 0.39 (0.16 ± 0.01) and 70.84 ± 47

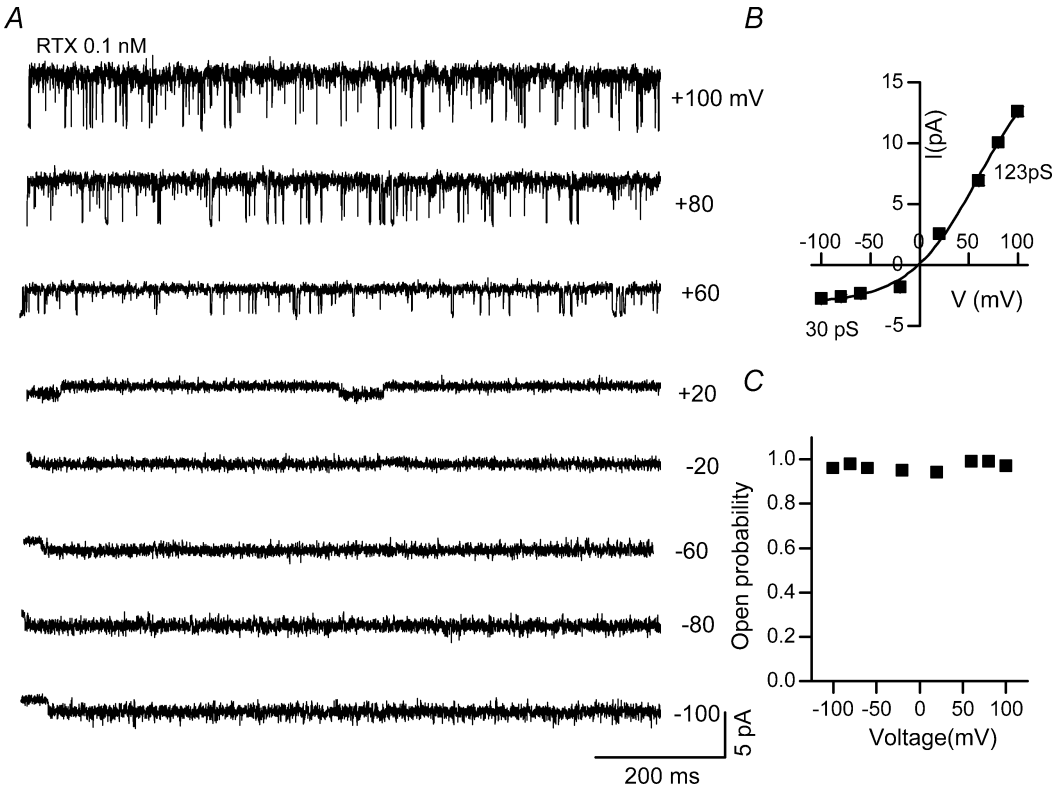

Figure 6. Voltage dependence of RTX-induced single channel activity in cell-attached patches from DRG neurones

A, single-channel current recordings at different membrane potentials from −100 to +100 mV in the presence of RTX (0.1 nM) in the pipette solution. *B*, current–voltage relationship showing outward rectification: slope conductance at −60 and +60 mV are 30 and 123 pS, respectively. *C*, single-channel P_o at different membrane potentials.

(0.04 ± 0.009) (Fig. 8*B* left panel and Table 1). Analyses of closed-time distributions reveal that in the presence of RTX, almost all of the events could be fitted with only two exponential components. The two shortest closed time constants were similar to the values obtained in the presence of capsaicin irrespective of the concentration and patch configuration, suggesting that these time constants represent fully liganded closed states (Premkumar *et al.* 2002). The fractional areas of distribution of the longer closed-time constants in the presence of RTX were negligible and significantly different from those in the presence of capsaicin ($P < 0.05$).

Ability of RTX and capsaicin to cause membrane depolarization and generate action potentials

To attribute a physiological significance to the slow and irreversible action of RTX, we recorded membrane depolarization in current-clamp conditions. Action potentials in response to a current injection (10–100 pA) were recorded in order to confirm that the neurones were excitable (inset to Fig. 9*A* and *B*). The average membrane potential was -57.1 ± 1 mV ($n = 42$). Capsaicin induced a dose-dependent depolarization and when it reached threshold it generated bursts of action potentials. At lower concentrations of capsaicin (< 30 nM), the depolarization did not reach the threshold to fire action potentials (data not shown). Capsaicin (30 nM) induced a depolarization of 13.3 ± 3.5 mV ($n = 7$, Fig. 9*A* and *C*). The extent of membrane depolarization induced by lower concentrations of RTX was similar to that seen with capsaicin (3 pM, 10.6 ± 1.6 mV, $n = 6$; 10 pM, 14.1 ± 1.5 mV, $n = 10$; 100 pM, 16.3 ± 3 mV, $n = 8$). Higher concentrations of RTX induced greater depolarization (10 nM, 32.2 ± 5.1 mV, $n = 5$; 1 μM, 52 ± 2 mV, $n = 3$) (Fig. 9*C*).

Capsaicin (30 nM) generated a significantly greater ($P < 0.05$) number of action potentials (54.2 ± 10.5) as compared to lower concentrations of RTX (3 pM, 16.6 ± 8.3, $n = 6$; 10 pM, 24.6 ± 6.9, $n = 10$). At intermediate concentrations ($\sim$100 pM) there was an increase in the number of action potentials (77.8 ± 11.8, $n = 8$).

At higher concentrations (10 nM–1 μM) of RTX there was a decrease in the number of action potentials probably due to rapid and sustained depolarization (10 nM,

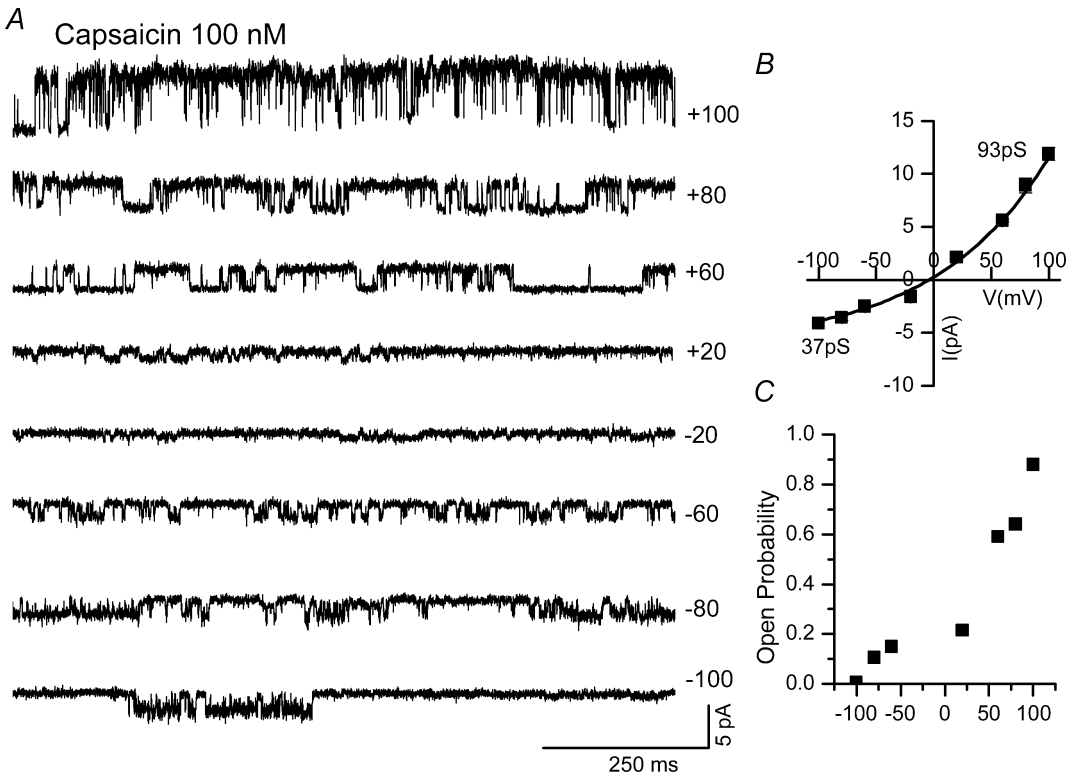

Figure 7. Voltage dependence of capsaicin-induced single channel activity in cell-attached patches from DRG neurones
A, single-channel current recording from -100 to $+100$ mV in the presence of capsaicin (100 nM). *B*, current–voltage relationship showing outward rectification: slope conductance at -60 and $+60$ mV are 41 and 93 pS, respectively. *C*, single-channel P_o at different membrane potentials, showing a steep voltage-dependent decrease at negative potentials.

Table 1. Open and closed time distribution of RTX- and capsaicin-induced currents

				Open time				Closed time			
V_m (mV)	n	P_o	Conc. (nM)	τ_1	τ_2	τ_3	τ_4	τ_1	τ_2	τ_3	τ_4
RTX											
−60	6	0.94 ± 0.02	0.1	0.46 ± 0.1 (0.03 ± 0.01)	5.57 ± 2.4 (0.5 ± 0.3)	10.2 ± 1.8 (0.47 ± 0.3)	— —	0.05 ± 0.007 (0.47 ± 0.02)	0.12 ± 0.005 (0.5 ± 0.02)	1.1 ± 0.26 (0.01 ± 0.002)	— —
+60	3	0.98 ± 0.02	0.1	1.6 ± 1.2 (0.11 ± 0.1)	6.58 ± 0.56 (0.72 ± 0.12)	12 ± 1 (0.25 ± 0.01)	— —	0.1 ± 0.008 (0.89 ± 0.02)	0.46 ± 0.02 (0.08 ± 0.01)	8.7 ± 3.9 (0.01 ± 0.01)	— —
CAP											
−60	6	0.1 ± 0.04	100	0.11 ± 0.01 (0.26 ± 0.05)	0.76 ± 0.18 (0.49 ± 0.07)	2.61 ± 0.84 (0.34 ± 0.08)	— —	0.13 ± 0.02 (0.43 ± 0.04)	0.79 ± 0.12 (0.31 ± 0.03)	3.47 ± 0.59 (0.19 ± 0.03)	30.8 ± 12.4 (0.04 ± 0.02)
+60	7	0.53 ± 0.04	100	0.14 ± 0.04 (0.11 ± 0.02)	0.7 ± 0.13 (0.28 ± 0.03)	3.83 ± 0.62 (0.44 ± 0.02)	14.7 ± 2.6 (0.13 ± 0.03)	0.06 ± 0.02 (0.39 ± 0.04)	0.67 ± 0.39 (0.4 ± 0.03)	1.66 ± 0.39 (0.16 ± 0.01)	70.84 ± 47 (0.04 ± 0.009)

24.5 ± 8.6, $n = 5$; 1 μM, 14.6 ± 4.6, $n = 3$) (Fig. 9*D*). Even though RTX induced a concentration-dependent change in the membrane potential, its effect on the number of action potentials followed a bell-shaped curve with highest activity being induced by intermediate concentrations (∼100 pM). Thus, lower concentrations of RTX can be potentially used to induce depolarization, which might be sufficient to induce a sustained Ca^{2+} influx (due to its irreversible nature) that could lead to neuronal degeneration over time and contribute to its clinical usefulness. These results suggest that because of its ultrapotent nature, low concentrations of RTX can cause a sustained activation of TRPV1 without generating action potentials, preventing the nociceptive information from reaching the brain. A similar phenomenon occurring at the nerve terminals innervating the bladder could explain why intravesicular administration of RTX causes less discomfort/pain during the treatment for bladder hyper-reflexia.

Discussion

In this study we confirm that RTX is a potent agonist of TRPV1 and that the whole-cell current response and single-channel current activity cannot be reversed readily, consistent with its high affinity for the receptor (Szallasi & Blumberg, 1990*b*; Caterina *et al.* 1997). This property of RTX has proven to be a useful tool to study interactions of agonists and antagonists with TRPV1 in receptor-binding experiments using its tritiated form. It is interesting that despite being an ultrapotent agonist with very high affinity, several weaker agonists can displace RTX from its binding site over time. Several studies have identified residues in the extracellular and intracellular domains that are involved in RTX binding (Jung *et al.* 1999, 2002; Chou *et al.* 2004; Gavva *et al.* 2004). The dichotomy between affinity and functional effects shown by some studies raises interesting questions about the functional relevance of residues identified as critical for RTX and capsaicin binding (Gavva *et al.* 2004). It also underscores the importance and relevance of the action of RTX on TRPV1, especially in light of its usefulness for certain painful conditions (Helyes *et al.* 2004) including urinary bladder hyper-reflexia (Giannantoni *et al.* 2004; Palma *et al.* 2004).

Although RTX is a potent agonist, the rate of activation of TRPV1 current is slower than with capsaicin and protons. Binding sites for capsaicin and RTX have been identified in the cytosolic and transmembrane domains of the channel, and the lipophilicity of the agonist affecting the ability of the drug to cross the membrane and interact with its respective binding site(s) might contribute to the differences observed in the activation kinetics (Jung *et al.* 1999, 2002; Chou *et al.* 2004; Vyklicky *et al.* 2003). Low-potency agonists, such as olvanil and capsiate, have been shown to exhibit low pungency, which is attributed partly to their high lipophilicity. Subcutaneous administration of these low-potency agonists induced nocifensive behaviour; however, no effect was seen when they were applied on the skin or mucous membranes (Iida *et al.* 2003; Neubert *et al.* 2003). This discrepancy might be in part due to low levels of the agonists being able to access the nerve terminals when applied superficially. In some *in vivo* studies, RTX induced an increase in the threshold for paw withdrawal latency in the hot plate test (Szabo *et al.* 1999; Almasi *et al.* 2003); however, nocifensive behaviour was observed in other studies, which used eye wipe test (Szallasi & Blumberg, 1989). Furthermore, intravesicular administration of RTX did not induce suprapubic discomfort, unlike that seen following capsaicin administration (Giannantoni *et al.* 2002). These findings are consistent with the observation that the ability of RTX to induce action potentials follows a bell-shaped curve, in that there was a significant increase in the number of action potentials only at intermediate concentrations (Fig. 9). The property of slow activation may be relevant as the receptor potential is changed in a ramp-like fashion, which is not rapid enough to induce a concerted activation of voltage-gated Na^+ channels to generate an action potential at the nerve terminal. This property might contribute to the lack of painful burning sensation with RTX, which is observed with capsaicin. Moreover, the RTX-induced response is long lasting; therefore much lower concentrations of the drug than

are being used currently (50–100 nM) could potentially be used to achieve maximal activation of the receptor over a period of time in a therapeutically safe manner while avoiding potential side effects due to systemic absorption (Giannantoni *et al.* 2004; Palma *et al.* 2004). Current clinical trials for bladder hyper-reflexia are being conducted to determine the most effective concentration of RTX and the duration of its application for optimum clinical benefits (Lazzeri *et al.* 2004*a*,*b*; Payne *et al.* 2005). Vanilloid agonists exhibit different potencies for receptor binding and Ca^{2+} uptake assays (Acs *et al.* 1995; Walpole *et al.* 1996). RTX was found to be 25-fold more potent for binding (K_d, 40 pM) as compared to its ability to induce Ca^{2+} uptake (K_d, 1.0 nM) (Acs *et al.* 1995). An EC_{50} of 270 nM was determined for capsaicin when Ca^{2+} influx was used as a parameter. However, [^{3}H]RTX binding was inhibited by capsaicin with a 10-fold lower affinity (K_d, 3 μM) (Acs *et al.* 1995). It was postulated that two different types of vanilloid receptors could be mediating these distinct responses (Szallasi & Blumberg, 1996; Biro *et al.* 1997). These were denoted as R-type and C-type vanilloid receptors. However, both R- and C-type responses could be seen in cell lines that expressed cloned vanilloid receptor TRPV1, ruling out the possibility of two different receptor types.

While determining the potency of RTX and capsaicin to activate TRPV1 current, it was found that RTX was 20-fold more potent (EC_{50}, 39 nM) than capsaicin (EC_{50}, 710 nM)

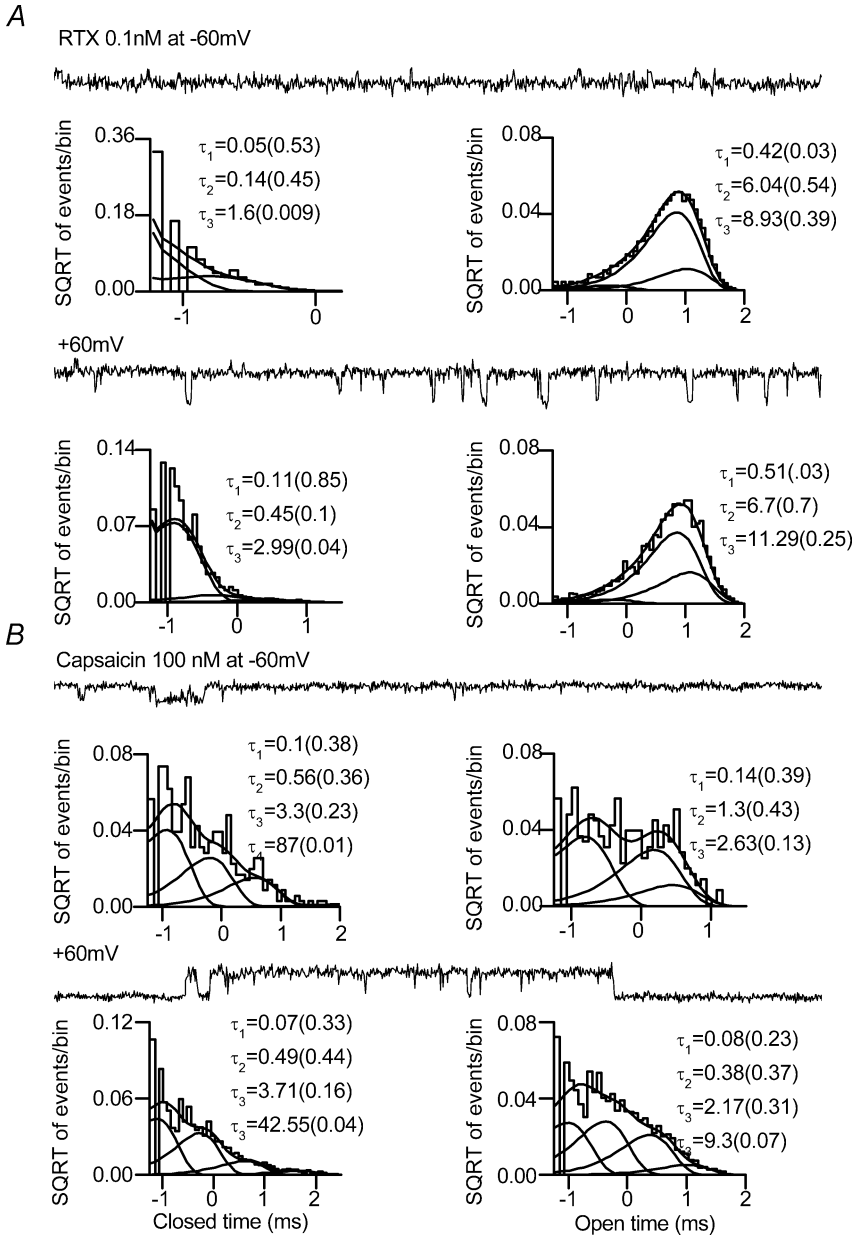

Figure 8. Single-channel kinetics of TRPV1 channel activity induced by RTX and capsaicin in cell-attached patches from DRG neurones
A, open- and closed-time distributions in the presence of RTX (0.1 nM) at −60 mV and +60 mV; open and closed time could be well-fitted with three exponential components. The time constants and the relative areas of distribution (in parenthesis) are shown. *B*, at −60 mV, in the presence of capsaicin (100 nM) the closed-time distribution is well-fitted with four exponential components and the open-time distribution is well-fitted with three exponential components. At +60 mV, the closed- and open-time distributions are well fitted with four exponential components. In the presence of RTX, the channel predominantly dwelled in the longer open states the majority of the time as compared to activation by capsaicin.

(Caterina *et al.* 1997). In TRPV1 transfected human embryonic kidney (HEK293) cells, capsaicin activated a current with an EC_{50} of 110 nM (Tominaga *et al.* 1998). In this study, we have found that a meaningful dose–response curve can not be constructed because repeated application of submaximal concentration of RTX induced larger currents until a maximal response was attained. Although RTX is a potent agonist, the activation of the current is slower than with capsaicin, and it deactivates minimally. The high potency is indicated by the minimal deactivation of the whole-cell currents, which is a result of its high affinity for the channel. The presence of critical intracellular residues, which need to be accessed by passing through the membrane, might be one of the contributing factors for the slow activation kinetics of RTX-induced membrane currents. It is also possible that RTX has both agonistic and antagonistic actions and therefore acts as a partial agonist. This is conceivable given the finding that iodoRTX is a potent antagonist of TRPV1. To better understand the nature of activation of TRPV1 by

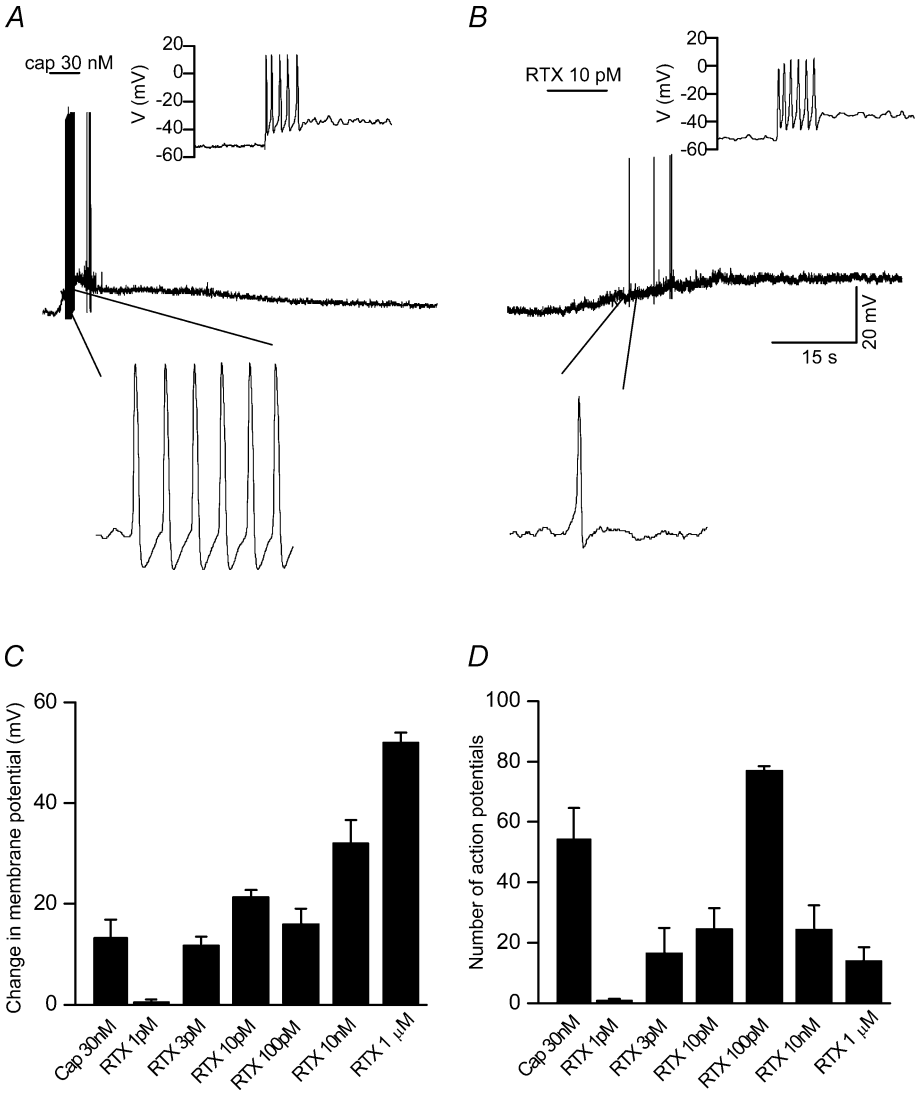

Figure 9. RTX- and capsaicin-induced membrane depolarization and the ability to generate action potentials

A, capsaicin-induced (30 nM) membrane depolarization resulted in a burst of action potentials. Inset shows action potentials in response to current injection. *B*, RTX-induced (10 pM) membrane depolarization, which is slow and sustained and generated a few action potentials. Note that the membrane potential does not reach baseline even after washout. Inset shows action potentials in response to current injection. Representative regions are shown in expanded timescale below. *C*, summary graph showing the extent of membrane depolarization induced by capsaicin (30 nM) and different concentrations of RTX (1 pM–1 μM). *D*, summary graph showing the number of action potentials induced following application of capsaicin and RTX.

RTX, we have characterized the single-channel properties of RTX- and capsaicin-induced channel activity.

We have used cell-attached and excised patch configurations to record single-channel currents activated by RTX and compared the properties with single-channel currents activated by capsaicin. A clear dose-dependent increase in P_o was not observed with RTX; only the time to reach the maximal P_o decreased with increasing concentrations. A concentration of 0.1–0.2 nM could maximally activate the receptor. Furthermore, there was no voltage-dependent change in P_o with RTX, whereas capsaicin-induced current shows a steep voltage-dependent decrease in P_o at negative potentials, which is consistent with earlier work (Premkumar *et al.* 2002; Voets *et al.* 2004). It is possible that binding of capsaicin is voltage dependent, which is reflected as a reduction in P_o. Despite maximal activation of the receptor by RTX, single-channel conductance shows clear outward rectification. The lesser extent of RTX-induced whole-cell current rectification could be due to a lack of voltage-dependent reduction in P_o at negative membrane potentials. As maximal activation of TRPV1 by RTX occurs even at low concentrations, it provides a means of studying the gating properties without interference from binding events, in that the equilibrium is greatly favoured towards the open state. Therefore, we were able to separate the gating events from binding events to study kinetics in detail. Open-time distributions show that the time constants are longer and that their areas of distribution are greater in the presence of RTX than in the presence of capsaicin. The channel predominantly dwelled in the longer open states as reflected by the fractional area of distribution (Fig. 8). Also, consistent with the high mean open times and P_o, the closed-time distribution could be fitted in most patches with only two exponential components, and even if a third exponential component was required, the area of its distribution was negligible.

It is clear that the concentrations of RTX and capsaicin that brought the membrane potentials rapidly to threshold, generated action potentials. With lower concentrations of capsaicin, the membrane potential did not even reach the threshold. On the other hand, very low concentrations of RTX, given its irreversible nature, induced a sustained depolarization and changed the membrane potential in a ramp-like fashion beyond the threshold, and yet it either failed to generate, or generated few action potentials in some cells. There are two advantages of using RTX. First, because of its irreversible nature, very low concentrations (well below the toxic levels) could be applied locally. Second, slow and sustained depolarization results in a gradual inactivation of voltage-gated Na^+ channels causing a depolarization block, which prevents action potential generation. However, at the same time RTX can sufficiently increase intracellular Ca^{2+} levels via TRPV1 to induce nerve terminal death for pain relief. As the nerve terminals have the ability to regenerate, long-term toxicity may not be a major concern.

It is important to understand the properties of RTX-induced TRPV1 currents because of its potential usefulness as a therapeutic agent. RTX is currently undergoing clinical trials, and showing beneficial effects in rodent models, for the treatment of bladder hyper-reflexia. A single intravesicular or intra-articular administration of RTX produces a long-lasting amelioration of the condition (Brady *et al.* 2004; Helyes *et al.* 2004). Its long-term beneficial effects are induced by sustained activation of TRPV1, potentially increasing intracellular Ca^{2+} levels, which subsequently induces nerve terminal death (Cruz *et al.* 1997; Lazzeri *et al.* 1998; Giannantoni *et al.* 2002; Brady *et al.* 2004; Karai *et al.* 2004; Lazzeri *et al.* 2004*b*,*c*). Slow and sustained activation at lower concentrations might contribute to the lack of pungency of RTX, as compared to capsaicin, which favours its usefulness during intravesicular administration.

References

Acs G, Lee J, Marquez VE, Wang S, Milne GW, Du L *et al.* (1995). Resiniferatoxin-amide and analogues as ligands for protein kinase C and vanilloid receptors and determination of their biological activities as vanilloids. *J Neurochem* **65**, 301–318.

Almasi R, Petho G, Bolcskei K & Szolcsanyi J (2003). Effect of resiniferatoxin on the noxious heat threshold temperature in the rat: a novel heat allodynia model sensitive to analgesics. *Br J Pharmacol* **139**, 49–58.

Baccei ML, Bardoni R & Fitzgerald M (2003). Development of nociceptive synaptic inputs to the neonatal rat dorsal horn: glutamate release by capsaicin and menthol. *J Physiol* **549**, 231–242.

Birder LA, Nakamura Y, Kiss S, Nealen ML, Barrick S, Kanai AJ *et al.* (2002). Altered urinary bladder function in mice lacking the vanilloid receptor TRPV1. *Nat Neurosci* **5**, 856–860.

Biro T, Acs G, Acs P, Modarres S & Blumberg PM (1997). Recent advances in understanding of vanilloid receptors: a therapeutic target for treatment of pain and inflammation in skin. *J Investig Dermatol Symp Proc* **2**, 56–60.

Brady CM, Apostolidis AN, Harper M, Yiangou Y, Beckett A, Jacques TS, Freeman A, Scaravilli F, Fowler CJ & Anand P (2004). Parallel changes in bladder suburothelial vanilloid receptor TRPV1 and pan-neuronal marker PGP9.5 immunoreactivity in patients with neurogenic detrusor overactivity after intravesical resiniferatoxin treatment. *BJU Int* **93**, 770–776.

Caterina MJ & Julius D (2001). The vanilloid receptor: a molecular gateway to the pain pathway. *Annu Rev Neurosci* **24**, 487–517.

Caterina MJ, Leffler A, Malmberg AB, Martin WJ, Trafton J, Petersen-Zeitz KR *et al.* (2000). Impaired nociception and pain sensation in mice lacking the capsaicin receptor. *Science* **288**, 306–313.

Caterina MJ, Schumacher MA, Tominaga M, Rosen TA, Levine JD & Julius D (1997). The capsaicin receptor: a heat-activated ion channel in the pain pathway. *Nature* **389**, 816–824.

Chou MZ, Mtui T, Gao YD, Kohler M & Middleton RE (2004). Resiniferatoxin binds to the capsaicin receptor (TRPV1) near the extracellular side of the S4 transmembrane domain. *Biochemistry* **43**, 2501–2511.

Chuang HH, Prescott ED, Kong H, Shields S, Jordt SE, Basbaum AI *et al.* (2001). Bradykinin and nerve growth factor release the capsaicin receptor from PtdIns $(4,5)P_2$-mediated inhibition. *Nature* **411**, 957–962.

Chung SH, Moore JB, Xia LG, Premkumar LS & Gage PW (1990). Characterization of single channel currents using digital signal processing techniques based on Hidden Markov Models. *Philos Trans R Soc Lond B Biol Sci* **329**, 265–285.

Cruz F, Guimaraes M, Silva C, Rio ME, Coimbra A & Reis M (1997). Desensitization of bladder sensory fibers by intravesical capsaicin has long lasting clinical and urodynamic effects in patients with hyperactive or hypersensitive bladder dysfunction. *J Urol* **157**, 585–589.

Davis JB, Gray J, Gunthorpe MJ, Hatcher JP, Davey PT, Overend P *et al.* (2000). Vanilloid receptor-1 is essential for inflammatory thermal hyperalgesia. *Nature* **405**, 183–187.

De Petrocellis L, Harrison S, Bisogno T, Tognetto M, Brandi I, Smith GD *et al.* (2001). The vanilloid receptor (TRPV1)-mediated effects of anandamide are potently enhanced by the cAMP-dependent protein kinase. *J Neurochem* **77**, 1660–1663.

Dinh QT, Groneberg DA, Peiser C, Mingomataj E, Joachim RA, Witt C *et al.* (2004). Substance P expression in TRPV1 and trkA-positive dorsal root ganglion neurons innervating the mouse lung. *Respir Physiol Neurobiol* **144**, 15–24.

Dinis P, Charrua A, Avelino A, Yaqoob M, Bevan S, Nagy I *et al.* (2004). Anandamide-evoked activation of vanilloid receptor 1 contributes to the development of bladder hyperreflexia and nociceptive transmission to spinal dorsal horn neurons in cystitis. *J Neurosci* **24**, 11253–11263.

Docherty RJ, Yeats JC, Bevan S & Boddeke HW (1996). Inhibition of calcineurin inhibits the desensitization of capsaicin-evoked currents in cultured dorsal root ganglion neurones from adult rats. *Pflugers Arch* **431**, 828–837.

Doyle MW, Bailey TW, Jin YH & Andresen MC (2002). Vanilloid receptors presynaptically modulate cranial visceral afferent synaptic transmission in nucleus tractus solitarius. *J Neurosci* **22**, 8222–8229.

Gavva NR, Klionsky L, Qu Y, Shi L, Tamir R & Edenson S (2004). Molecular determinants of vanilloid sensitivity in TRPV1. *J Biol Chem* **279**, 20283–20295.

Giannantoni A, Di Stasi SM, Stephen RL, Bini V, Costantini E & Porena M (2004). Intravesical resiniferatoxin versus botulinum-A toxin injections for neurogenic detrusor overactivity: a prospective randomized study. *J Urol* **172**, 240–243.

Harvey JS, Davis C, James IF & Burgess GM (1995). Activation of protein kinase C by the capsaicin analogue resiniferatoxin in sensory neurones. *J Neurochem* **65**, 1309–1317.

Helyes Z, Szabo A, Nemeth J, Jakab B, Pinter E, Banvolgyi A, Kereskai L, Keri G & Szolcsanyi J (2004). Antiinflammatory and analgesic effects of somatostatin released from capsaicin-sensitive sensory nerve terminals in a Freund's adjuvant-induced chronic arthritis model in the rat. *Arthritis Rheum* **50**, 1677–1685.

Huang SM, Bisogno T, Trevisani M, Al-Hayani A, De Petrocellis L, Fezza F *et al.* (2002). An endogenous capsaicin-like substance with high potency at recombinant and native vanilloid TRPV1 receptors. *Proc Natl Acad Sci U S A* **99**, 8400–8405.

Hwang SW, Cho H, Kwak J, Lee SY, Kang CJ, Jung J *et al.* (2000). Direct activation of capsaicin receptors by products of lipoxygenases: endogenous capsaicin-like substances. *Proc Natl Acad Sci U S A* **97**, 6155–6160.

Iida T, Moriyama T, Kobata K, Morita A, Murayama N, Hashizume S, Fushiki T, Yazawa S, Watanabe T & Tominaga M (2003). TRPV1 activation and induction of nociceptive response by a non-pungent capsaicin-like compound, capsiate. *Neuropharmacology* **44**, 958–967.

Julius D & Basbaum AI (2001). Molecular mechanisms of nociception. *Nature* **413**, 203–210.

Jung J, Hwang SW, Kwak J, Lee SY, Kang CJ, Kim WB, Kim D & Oh U (1999). Capsaicin binds to the intracellular domain of the capsaicin-activated ion channel. *J Neurosci* **19**, 529–538.

Jung J, Lee SY, Hwang SW, Cho H, Shin J, Kang YS *et al.* (2002). Agonist recognition sites in the cytosolic tails of vanilloid receptor 1. *J Biol Chem* **277**, 44448–44454.

Karai L, Brown DC, Mannes AJ, Connelly ST, Brown J, Gandal M *et al.* (2004). Deletion of vanilloid receptor 1-expressing primary afferent neurons for pain control. *J Clin Invest* **113**, 1344–1352.

Kim JH, Rivas DA, Shenot PJ, Green B, Kennelly M, Erickson JR *et al.* (2003). Intravesical resiniferatoxin for refractory detrusor hyperreflexia: a multicenter, blinded, randomized, placebo-controlled trial. *J Spinal Cord Med* **26**, 358–363.

Koplas PA, Rosenberg RL & Oxford GS (1997). The role of calcium in the desensitization of capsaicin responses in rat dorsal root ganglion neurons. *J Neurosci* **17**, 3525–3537.

Lazzeri M, Beneforti P & Turini D (1998). Urodynamic effects of intravesical resiniferatoxin in humans: preliminary results in stable and unstable detrusor. *J Urol* **158**, 2093–2096.

Lazzeri M, Spinelli M, Beneforti P, Malaguti S, Giardiello G & Turini D (2004*a*). Intravesical infusion of resiniferatoxin by a temporary in situ drug delivery system to treat interstitial cystitis: a pilot study. *Eur J Urol* **45**, 98–102.

Lazzeri M, Spinelli M, Zanollo A & Turini D (2004*b*). Intravesical vanilloids and neurogenic incontinence: ten years experience. *Urol Int* **72**, 145–149.

Lazzeri M, Vannucchi MG, Zardo C, Spinelli M, Beneforti P, Turini D *et al.* (2004*c*). Immunohistochemical evidence of vanilloid receptor 1 in normal human urinary bladder. *Eur Urol* **46**, 792–798.

Linard C, Marquette C, Strup C, Aigueperse J & Mathe D (2003). Involvement of primary afferent nerves after abdominal irradiation: consequences on ileal contractile activity and inflammatory mediator release in the rat. *Dig Dis Sci* **48**, 688–697.

Lundberg JM, Martling CR & Saria A (1983). Substance P and capsaicin-induced contraction of human bronchi. *Acta Physiol Scand* **119**, 49–53.

Marinelli S, Di Marzo V, Berretta N, Matias I, Maccarrone M, Bernardi G *et al.* (2003). Presynaptic facilitation of glutamatergic synapses to dopaminergic neurons of the rat substantia nigra by endogenous stimulation of vanilloid receptors. *J Neurosci* **23**, 3136–3144.

Marinelli S, Vaughan CW, Christie MJ & Connor M (2002). Capsaicin activation of glutamatergic synaptic transmission in the rat locus coeruleus *in vitro*. *J Physiol* **543**, 531–540.

Marshall IC, Owen DE, Cripps TV, Davis JB, McNulty S & Smart D (2003). Activation of vanilloid receptor 1 by resiniferatoxin mobilizes calcium from inositol 1,4,5-trisphosphate-sensitive stores. *Br J Pharmacol* **138**, 172–176.

Mitchell JA, Williams FM, Williams TJ & Larkin SW (1997). Role of nitric oxide in the dilator actions of capsaicin-sensitive nerves in the rabbit coronary circulation. *Neuropeptides* **31**, 333–338.

Nakatsuka T, Furue H, Yoshimura M & Gu JG (2002). Activation of central terminal vanilloid receptor-1 receptors and alpha beta-methylene-ATP-sensitive P2X receptors reveals a converged synaptic activity onto the deep dorsal horn neurons of the spinal cord. *J Neurosci* **22**, 1228–1237.

Neubert JK, Karai L, Jun JH, Kim HS, Olah Z & Iadarola MJ (2003). Peripherally induced resiniferatoxin analgesia. *Pain* **104**, 219–228.

Oroszi G, Szilvassy Z, Nemeth J, Tosaki A & Szolcsanyi J (1999). Interplay between nitric oxide and CGRP by capsaicin in isolated guinea-pig heart. *Pharmacol Res* **40**, 125–128.

Palma PC, Thiel M, Riccetto CL, Dambros M, Miyaoka R & Netto NR Jr (2004). Resiniferatoxin for detrusor instability refractory to anticholinergics. *Int Braz J Urol* **30**, 53–58.

Payne CK, Mosbaugh PG, Forrest JB, Evans RJ, Whitmore KE, Antoci JP *et al.* (2005). Intravesical resiniferatoxin for the treatment of interstitial cystitis: a randomized, double-blind, placebo controlled trial. *J Urol* **173**, 1590–1594.

Premkumar LS, Agarwal S & Steffen D (2002). Single-channel properties of native and cloned rat vanilloid receptors. *J Physiol* **545**, 107–117.

Premkumar LS, Qi ZH, Van Buren J & Raisinghani M (2004). Enhancement of potency and efficacy of NADA by PKC-mediated phosphorylation of vanilloid receptor. *J Neurophysiol* **91**, 1442–1449.

Premkumar LS, Qin F & Auerbach A (1997). Subconductance states of a mutant NMDA receptor channel kinetics, calcium, and voltage dependence. *J Gen Physiol* **109**, 181–189.

Qin F, Auerbach A & Sachs F (1996). Estimating single-channel kinetic parameters from idealized patch-clamp data containing missed events. *Biophys J* **70**, 264–280.

Roberts JC, Davis JB & Benham CD (2004). [3H]Resiniferatoxin autoradiography in the CNS of wild-type and TRPV1 null mice defines TRPV1 (TRPV1-1) protein distribution. *Brain Res* **995**, 176–183.

Szabo T, Biro T, Gonzalez AF, Palkovits M & Blumberg PM (2002). Pharmacological characterization of vanilloid receptor located in the brain. *Brain Res Mol Brain Res* **98**, 51–57.

Szabo T, Olah Z, Iadarola MJ & Blumberg PM (1999). Epidural resiniferatoxin induced prolonged regional analgesia to pain. *Brain Res* **840**, 92–98.

Szallasi A & Blumberg PM (1989). Resiniferatoxin, a phorbol-related diterpene, acts as an ultrapotent analog of capsaicin, the irritant constituent in red pepper. *Neuroscience* **30**, 515–520.

Szallasi A & Blumberg PM (1990*a*). Resiniferatoxin and its analogs provide novel insights into the pharmacology of the vanilloid (capsaicin) receptor. *Life Sci* **47**, 1399–1408.

Szallasi A & Blumberg PM (1990*b*). Specific binding of resiniferatoxin, an ultrapotent capsaicin analog, by dorsal root ganglion membranes. *Brain Res* **524**, 106–111.

Szallasi A & Blumberg PM (1996). Vanilloid receptors: new insights enhance potential as a therapeutic target. *Pain* **68**, 195–208.

Tominaga M, Caterina MJ, Malmberg AB, Rosen TA, Gilbert H, Skinner K *et al.* (1998). The cloned capsaicin receptor integrates multiple pain-producing stimuli. *Neuron* **21**, 531–543.

Van Buren JJ, Bhat S, Rotello R, Pauza ME & Premkumar LS (2005). Sensitization and translocation of TRPV1 by insulin and IGF-I. *Mol Pain* **1**, 17.

Vass Z, Dai CF, Steyger PS, Jancso G, Trune DR & Nuttall AL (2004). Co-localization of the vanilloid capsaicin receptor and substance P in sensory nerve fibers innervating cochlear and vertebro-basilar arteries. *Neuroscience* **124**, 919–927.

Voets T, Droogmans G, Wissenbach U, Janssens A, Flockerzi V & Nilius B (2004). The principle of temperature-dependent gating in cold- and heat-sensitive TRP channels. *Nature* **430**, 748–754.

Vyklicky L, Lyfenko A, Kuffler DP & Vlachova V (2003). Vanilloid receptor TRPV1 is not activated by vanilloids applied intracellularly. *Neuroreport* **14**, 1061–1065.

Walpole CS, Bevan S, Bloomfield G, Breckenridge R, James IF, Ritchie T *et al.* (1996). Similarities and differences in the structure-activity relationships of capsaicin and resiniferatoxin analogues. *J Med Chem* **39**, 2939–2952.

Zheng J, Dai C, Steyger PS, Kim Y, Vass Z, Ren T *et al.* (2003). Vanilloid receptors in hearing: altered cochlear sensitivity by vanilloids and expression of TRPV1 in the organ of corti. *J Neurophysiol* **90**, 444–455.

Zygmunt PM, Petersson J, Andersson DA, Chuang H, Sorgard M, Di Marzo V *et al.* (1999). Vanilloid receptors on sensory nerves mediate the vasodilator action of anandamide. *Nature* **400**, 452–457.

Acknowledgements

The TRPV1 clone was kindly provided by D. Julius (UCSF). This work was supported by grants from National Institutes of Health (NS042296 and DK065742) to L.S.P.